NEW RESULTS FROM H1 ON STRUCTURE FUNCTIONS

Vladimir SHEKELYAN (CHEKELIAN)

for the H1 Collaboration
DESY Hamburg / ITEP Moscow

New results on the proton structure functions are reported from the H1 experiment at HERA. The inclusive D^0 and $D^{*\pm}$ production in deep inelastic ep scattering is used for a first measurement of $F_2^{c\bar{c}}\left(x, Q^2\right)$ for Bjorken x between $8 \cdot 10^{-4}$ and $8 \cdot 10^{-3}$. In this kinematic range a ratio $F_2^{c\bar{c}}/F_2 = 0.237 \pm 0.021\,^{+0.043}_{-0.039}$ is observed. A precise measurement of the inclusive deep inelastic electron-proton cross section at momentum transfers $8.5 \leq Q^2 \leq 35$ GeV^2 and large inelasticity values $0.6 \leq y \leq 0.78$ is used to determine the longitudinal proton structure function F_L at HERA. Using a NLO QCD fit to the F_2 at lower y values, the F_2 contribution to the cross section at high y is subtracted and an average value of $F_L = 0.54 \pm 0.03(stat) \pm 0.22(syst)$ is obtained for $0.00013 \leq x \leq 0.00055$. Preliminary results on a measurement of the proton structure function $F_2(x, Q^2)$ are reported for Q^2 between 0.35 GeV^2 and 3.5 GeV^2 and for x values down to $6 \cdot 10^{-6}$ using data collected in 1995. The data represent an increase in kinematical range to lower x and Q^2 values of about a factor of 5, compared to previous H1 measurements. For the lowest Q^2 values F_2 is found to flatten off with x.

1 Introduction

The measurement of the inclusive deep inelastic lepton-proton scattering (DIS) cross section has been of great importance for the understanding of quark-gluon substructure of the proton. In the one-photon exchange approximation the inclusive scattering cross section is given by the expression

$$\frac{d^2\sigma}{dx dQ^2} = \frac{2\pi\alpha^2}{Q^4 x}\left(2 - 2y + \frac{y^2}{1+R}\right)F_2(x, Q^2) \quad (1)$$

Here Q^2 is the squared four-momentum transfer, x denotes the Bjorken scaling variable, and $y = Q^2/xs$ is the inelasticity, where s is the centre of mass energy squared of the collision. The structure function $F_2(x, Q^2)$ can be derived from the cross section, eq.(1), making an assumption for the ratio $R = F_2/2xF_1 - 1 = F_L/(F_2 - F_L)$, where the longitudinal proton structure function $F_L = F_2 - 2xF_1$ has not been measured yet at HERA.

Recently published measurements on the structure function F_2 at HERA based on analysis of the data taken in 1994 cover a wide range in Q^2, x, and y corresponding to $1.5 < Q^2 < 5000$ GeV^2, $3 \cdot 10^{-5} < x < 0.32$ and roughly $0.01 < y < 0.6$ [1,2].

New results on structure functions from the H1 experiment at HERA are presented in this paper. They cover the following three topics:

- a measurement of the charm contribution $F_2^{c\bar{c}}(x, Q^2)$ to the structure function of the proton which is sensitive to the gluon density $xg(x, Q^2)$ in the proton;
- a determination of the longitudinal proton structure function in the region of $8.5 \leq Q^2 \leq 35$ GeV^2 and small x values between $1.3 \cdot 10^{-4}$ and $5.5 \cdot 10^{-4}$
- an extension of the proton structure function measurements in a continuous way down to $Q^2 = 0.35$ GeV^2 and $x = 6 \cdot 10^{-6}$, the transition region between the deep inelastic approach and the photoproduction limit.

The data were recorded in 1994 and 1995 with the H1 detector, which is described in reference [3]. The incident electron energy was $E_e = 27.5$ GeV and the proton energy was $E_p = 820$ GeV, leading to a total centre of mass energy of the collision of $\sqrt{s} = 300$ GeV. A new calorimeter and tracking chamber with increased acceptance for small scattering angles have been installed in the winter shutdown 94/95. Together with a 70 cm shift of the main collision vertex in the proton direction, the data collected in 1995 have an acceptance in Q^2 down to $Q^2 \sim 0.3$ GeV^2. A feature of the HERA collider experiments is the possibility of measuring not only the scattered electron but also the complete hadronic final state, apart from losses near the beam pipe. This means that the kinematical variables x, y and Q^2 can be determined with complementary methods which experimentally are sensitive to different systematic effects. Furthermore the hadronic final state can be studied in detail.

2 Charm Contribution $F_2^{c\bar{c}}(x,Q^2)$ to the Proton Structure Function

The data used in this analysis have been collected in 1994 and correspond to an integrated luminosity of 2.97 ± 0.04 pb^{-1}. Tagging of charm events is performed by reconstructing D^0 and D^{*+} mesons[a] via their decays into $D^0 \to K^-\pi^+$ and $D^{*+} \to D^0\pi_s^+ \to (K^-\pi^+)\pi_s^+$, respectively. A satisfactory suppression of the combinatorial background is obtained by making use of the hard fragmentation of charm quarks. Furthermore, for the D^{*+} analysis the mass difference $\Delta m = m(D^{*+}) - m(D^0)$, being very close to the π^+ mass, leads to a better resolution and signal to background ratio than the D^{*+} mass itself. In Fig. 1 the inclusive D^0 and D^{*+} signals are shown. Fits to the data result in inclusive yields of 144 ± 19 D^0 and 103 ± 13 D^{*+} mesons with 8 ± 3 events being common to both analysis.

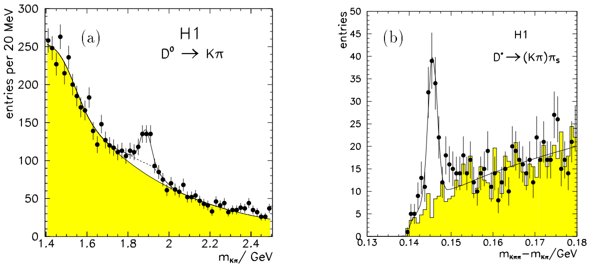

Figure 1: *Distribution (a) of $m_{K\pi}$ from the D^0 analysis and (b) of Δm from the D^{*+} analysis by requiring $|m_{K\pi} - m_{D^0}| < 90$ MeV. The shaded areas show the background expectations. The full lines are results of fits to the data.*

The charm contribution $F_2^{c\bar{c}}(x,Q^2)$ to the structure function is obtained by applying the expression for the one photon exchange cross section, eq.(1), for charm production with the assumption that the Callan-Gross relation holds, i.e. $R = F_2/2xF_1 - 1 = 0$. Figure 2 shows $F_2^{c\bar{c}}(x,Q^2)$ as measured by H1 together with the EMC results [4]. The present measurement extends our knowledge of $F_2^{c\bar{c}}(x,Q^2)$ by two orders of magnitude towards smaller x values: $8 \cdot 10^{-4} < x < 8 \cdot 10^{-3}$. Together with the EMC measurement a steep rise of $F_2^{c\bar{c}}$ is observed with decreasing x. An averaged over the kinematic range ratio $F_2^{c\bar{c}}/F_2 = 0.237 \pm 0.021\,^{+0.043}_{-0.039}$ is obtained.

In Fig.2 the data is also compared with NLO calculations [5] using the GRV-HO, the MRSH, and the MRSD0′ gluon densities and $m_c = 1.5$ GeV/c^2. MRSD0′ is still considered here, although the corresponding F_2 has already been excluded by inclusive measurements at HERA. Obviously it also fails to describe the charm production in DIS. The data also lie systematically above the other predictions. An agreement is observed between the measured $F_2^{c\bar{c}}$ and the NLO calculations based on the gluon density from the NLO QCD fit of H1 to the inclusive F_2 data [1]. The dominant theoretical uncertainty arises from the ignorance of m_c. It turns out that a change in m_c would affect the prediction and the measurement of $F_2^{c\bar{c}}$ nearly in the same way.

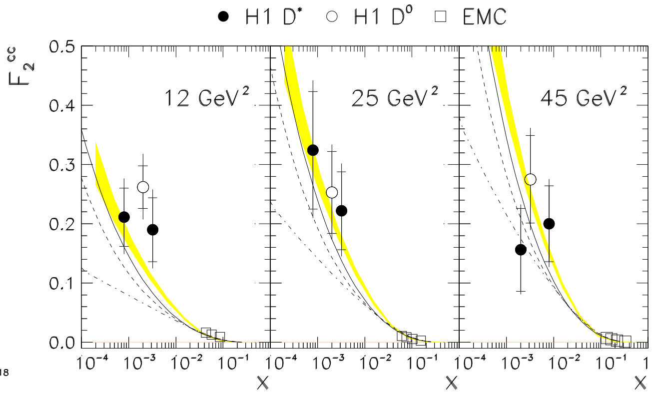

Figure 2: *$F_2^{c\bar{c}}$ as derived from the D^{*+} (full dots) and D^0 analysis (open circles) in comparison with NLO predictions using GRV-HO (full line), MRSH (dashed line) and MRSD0′ (dash-dotted line) and $m_c = 1.5$ GeV/c^2. The inner(outer) error bars refer to the statistical (total) errors. The shaded band represents the prediction from the NLO QCD fit to the F_2 measurements. The EMC data are also shown (open boxes).*

3 A Determination of the Longitudinal Proton Structure Function

The published H1 measurement [1] of F_2 was limited to y values below 0.6 and assumed a QCD calculation for F_L. At large y the weights of F_2 and F_L in eq.(1) become of comparable size. The H1 collaboration has attempted to reverse that procedure, i.e. to measure the cross section at the

[a] Charge conjugates are always implied.

maximum possible y and to derive F_L assuming that F_2 is given by a QCD fit to data at lower y. At HERA the measured y extends over about two orders of magnitude and F_2, combined with the high x data from muon scattering experiments, is described by standard perturbative QCD with a high level of accuracy. Thus the contribution of F_2 to the cross section can be determined from a NLO QCD fit to the data and subtracted from the measured cross section. The basic assumption of this procedure remains, until one has data at different HERA beam energies, that F_2 can indeed be extrapolated using QCD into the high y region, i.e. from lower to larger Q^2 at fixed x. This appears to be reasonable, given the impressive agreement of the F_2 measurements over 4 orders of magnitude in Q^2 with DGLAP QCD evolution.

The cross section measurement in the region $8.5 \leq Q^2 \leq 35$ GeV^2 and large inelasticity values $0.6 \leq y \leq 0.78$ was converted to a determination of F_L by subtracting the contribution of F_2. The latter is determined using the result of a NLO DGLAP QCD fit [1] to F_2 which was performed to data with $y < 0.35$, where the sensitivity to F_L is reduced. The radiative corrections were studied extensively. For example, by imposing the cut $y \geq 0.1$, with y reconstructed from the hadronic final state, a large part of the corrections is suppressed but the final result appears to be stable within about half of the statistical errors. The resulting F_L points in six bins of Q^2, or equivalently of x, are shown in Fig.3. The systematic errors are highly correlated from point to point and are very similar for all F_L values because they mainly depend on y. Thus the systematic error is drawn in Fig.3 as one error band of the width ± 0.22 around the central average F_L value $0.54 \pm 0.03 \pm 0.22$ which was obtained assuming F_L to be independent of x or Q^2 at constant y.

There are three main systematic error contributions which were carefully disentangled and studied:

- errors which affect only the high y cross section measurement, dominated by various cut efficiency errors and, at the lowest Q^2, by the photoproduction background uncertainty. These experimental errors amount to an absolute F_L error of about 0.16;

- those errors which are common to the cross section measurements at low and at high y, like the luminosity uncertainty. In the subtraction the effect of these errors is reduced to an F_L uncertainty of 0.03;

- errors of the subtracted F_2 contribution which arise from the experimental errors specific to the lower y region and from the fit assumptions like parametrizations and charm treatment. These errors were estimated to be about 0.14 including the residual dependence of the F_2 data at lower y on F_L.

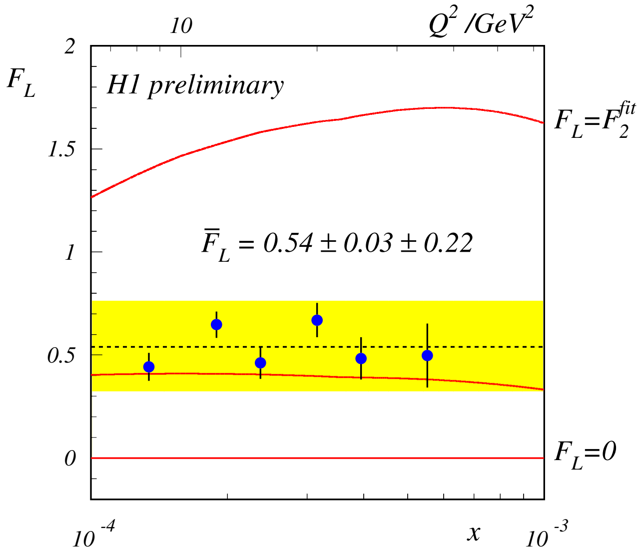

Figure 3: *Measured longitudinal structure function F_L for $y = 0.7$ as functions of x and of $Q^2 = sxy$ for $Q^2 = 8.5,\ 12,\ 15,\ 20,\ 25,\ 35\ GeV^2$. The error bars are the statistical error, the band is the systematic error common to all points. The lines $F_L = 0$ and $F_L = F_2$ represent the possible limits of F_L derived from the positivity of the cross sections of longitudinally and transversally polarized photons. The solid curve is a QCD calculation of F_L based on the F_2 data measured at lower y.*

Fig.3 shows the extreme limits of $F_L = 0$ and $F_L = F_2$ using the QCD fit. On average the measured F_L value is 2.6 standard deviations larger than zero and 4 to 5 standard deviations away from F_2. At low x the F_L structure function is related to the gluon distribution. The full line in Fig.3 represents the calculation of F_L according to the QCD relation [6,7] using the gluon (and quark) distributions determined by the QCD fit. There is consistency between the F_L values of this analysis and the gluon distribution determined from the scaling violations measured with F_2 in the low

y range.

4 A Measurement of the Proton Structure Function $F_2(x, Q^2)$ at Low x and Low Q^2

A data sample collected in 1995 was used to extend the proton structure function measurement to lower Q^2 and x values compared to the previous H1 analysis [1] (Q^2 from 1.5 GeV^2 to 0.35 GeV^2 and x from $3 \cdot 10^{-5}$ to $6 \cdot 10^{-6}$). For this data sample corresponding to an integrated luminosity of 120 nb^{-1} the interaction vertex was shifted by 70 cm in the proton direction. After an upgrade in the backward region of the H1 detector a lead/scintillating fiber calorimeter (SPACAL) [8] and a four module drift chamber (BDC) [8] are used for detecting scattering electrons. The new calorimeter has both an electromagnetic and hadronic section. The angular acceptance of the SPACAL is $153^0 < \theta < 177.8^0$ for collisions at the nominal vertex, increasing to 178.5^0 for collisions where the interaction vertex is shifted by 70 cm in the proton direction.

Deep inelastic scattering events are selected in which the most energetic cluster in SPACAL satisfies electron identification criteria and has energy larger than 7 GeV. A reconstructed interaction vertex from the tracker was required to be within 30 cm of the average vertex position along the beam (z) direction. Fig. 4 shows the energy and angular distribution of electron candidates in the DIS selected sample, together with Monte Carlo predictions for the sum of DIS and remaining photoproduction background. The Monte Carlo simulation is weighted with the measured structure function and normalized to the luminosity.

The kinematic variables of the inclusive scattering process $ep \to eX$ can be reconstructed in different ways using measured quantities from the hadronic final state and from the scattered electron. The application of different methods was important to check that the systematic errors were correctly evaluated. The basic formulae for Q^2 and y used in the different methods are given in reference [1]. As the main method the so-called "electron method" is used which is based on the scattered electron energy and angle. Lower y values are covered with the so-called "Σ method" which combines electron and hadronic information to reduce radiative corrections and calibration errors.

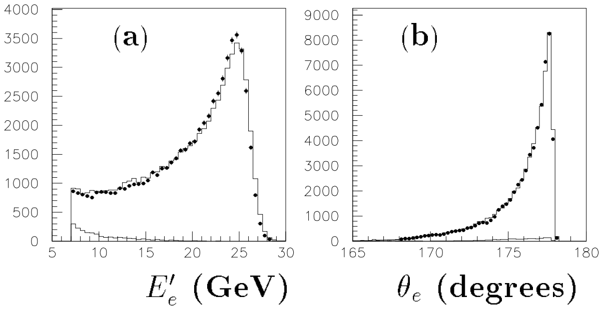

Figure 4: *Experimental (points) and Monte Carlo distributions of a) the energy of the scattered electron and b) the polar angle of the scattered electron for DIS events. The Monte Carlo curve is the sum of DIS and photoproduction events (shown separately by the lower curve).*

The structure function $F_2(x, Q^2)$ was derived after radiative corrections from the one-photon exchange cross section, eq.(1). The following assumption was taken for R in this analysis. For $Q^2 \geq 1$ GeV^2 R was calculated from the QCD relation [6,7] using the parton parametrization from the QCD fit. For the region $Q^2 < 1$ GeV^2 a VDM inspired function is used which interpolates between the value of R at $Q_o^2 = 1$ GeV^2 and $R = 0$ for $Q^2 = 0$

$$R = R(Q_o^2) \cdot Q^2/(Q^2 + m_\rho^2) \cdot (Q_o^2 + m_\rho^2)/Q_o^2 \quad (2)$$

where m_ρ^2 is the mass of the ρ meson.

For the final values of the structure function F_2 presented below, R was taken as described above for $Q^2 \geq 0.85$ GeV^2 and put to zero for smaller Q^2 values. Only the lowest x point in each Q^2 bin is affected significantly by R. For $Q^2 \geq 0.85$ GeV^2, the effect of R not being zero leads to a correction of about 10-15% at smallest x (and at most a few % elsewhere); for $Q^2 < 0.85$ GeV^2 assuming instead of $R = 0$, R as given by the prescription above, leads to an increase of F_2 for the lowest x points by approximately 10%.

A list of the systematics errors for F_2 with preliminary values is given below.

- A potential miscalibration of the electron energy in the SPACAL, varying from 1.5% at large electron energies to 3% at 8 GeV.
- 4% and 10% scale errors were assigned to the energy measurement of the hadronic final state in the liquid argon calorimeter and in the SPACAL, respectively.

- A shift of up to 1 mrad for the electron polar angle.
- The electron identification efficiency; vertex efficiency: 3%; BDC efficiency: 3%; trigger and timing veto: 0.5%.
- An error of up to 2% in the radiative correction.
- The uncertainty due to photoproduction background was assumed to be 30% of the correction applied, i.e. smaller than 6% of F_2. This affects only the highest y bins at lower Q^2.
- The total normalization uncertainty is 3% and results from the error on the luminosity and a correction for satellite bunches, which led to collisions about 70 cm displaced with respect to the main bunch.

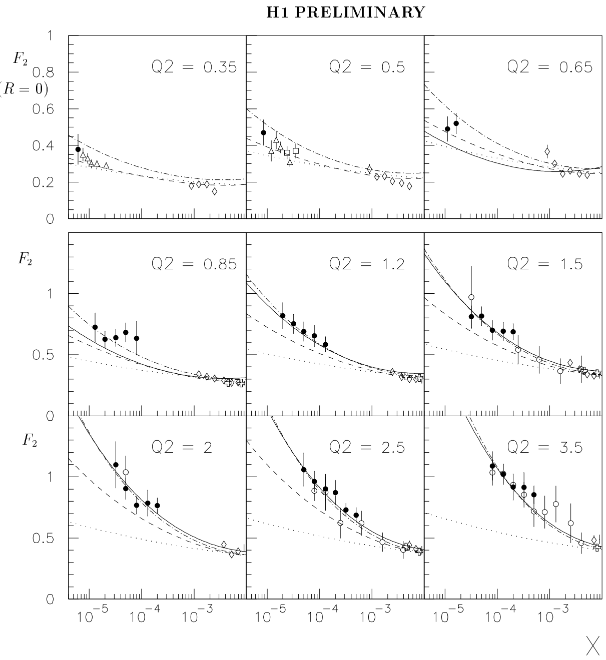

Figure 5: *Preliminary measurement of the proton structure function $F_2(x,Q^2)$ in the low Q^2 region by H1 (full points), together with the previous H1 results (open points) and results from the E665 experiment (open diamonds), NMC (open crosses) and ZEUS (open squares and triangles). Different predictions for F_2 are compared to the data: the model of Donnachie and Landshoff (dotted line), the CKMT model (dashed line), the model of Badelek and Kwiecinski (dashed doted line) and the model of Glück, Reya and Vogt (full line).*

In Fig. 5 the new data are compared with previous measurements of H1 [1], measurements of E665 [9], NMC [10] and ZEUS (preliminary)[11], and with predictions of models for F_2 at low x. The results are in good agreement with the previous H1 publication [1]. The data also show a smooth continuation from the fixed target measurements and are compatible with the preliminary ZEUS measurements [11]. It is seen that the rise of F_2 at low x is still present for $Q^2 \geq 0.85$ GeV^2, but becomes less steep for decreasing Q^2.

Parametrizations motivated by Regge theory relate the structure function to Reggeon exchange phenomena which successfully describe the slow rise of the total cross section with energy in hadron-hadron and γp interactions. Using the "bare" instead of the "effective" pomeron intercept, the CKMT [12] parametrization rises faster with x compared to former DOLA [13] calculations. Regge inspired models generally undershoot the data, except for the smallest Q^2 values where the calculations are in accord with the data. Some freedom exists in the CKMT model to improve the agreement with data in the region $Q^2 < 2$ GeV^2.

In Fig. 5 also the predictions from the QCD-based GRV model [6] are shown. This model assumes that all parton distributions at the very low $Q_0^2 = 0.34$ GeV^2 have a valence like shape, i.e. vanish for $x \to 0$. Assuming that the leading twist QCD evolution equations can be used to evolve the parton distributions from this low Q_0^2 scale to larger Q^2 values, GRV predicted that the structure function F_2 should rise towards low x even for low values of $Q^2 \sim 1$ GeV^2 [6]. Fig. 5 shows that the GRV distributions describe the data well for $Q^2 \geq 1$ GeV^2, but systematically undershoot the data for $Q^2 < 1$ GeV^2. Hence it turns out that the kinematic region studied here is a meeting ground for Regge inspired models, which describe the data at the low Q^2 end, and models based on pQCD, which account well for the high Q^2 end. The model of Badelek and Kwiecinski (BK [14]) combines the concepts of Vector Meson Dominance with dynamical parton models such as the GRV[6] parton distributions. It has by construction a smooth transition from pQCD to the real photon limit, that is in the region studied here. The BK model is found to describe the data.

5 Summary

Inclusive D^0 and $D^{*\pm}$ production in deep inelastic ep scattering is used for a first measurement of $F_2^{c\bar{c}}(x,Q^2)$ for $8\cdot10^{-4} \le x \le 8\cdot10^{-3}$. In this kinematic range a ratio $F_2^{c\bar{c}}/F_2 = 0.237 \pm 0.021\,^{+0.043}_{-0.039}$ is obtained. Consistency is observed between the measured $F_2^{c\bar{c}}$ and the result of the NLO QCD fit of H1 to the inclusive F_2 data.

An inclusive deep inelastic cross section measurement at y around 0.7 has been used to determine for the first time the longitudinal structure function $F_L(x,Q^2)$ at very low Bjorken x. The result is consistent with a higher order QCD calculation of F_L which essentially relied on the gluon distribution as determined by the F_2 scaling violations. The result excludes the extreme limits of $F_L = 0$ and $F_L = F_2$, corresponding to $R = 0$ and $R = \infty$, by 2.6 and 4.0-5.0 standard deviations, respectively. A determination of F_L at HERA which is free of any theoretical assumption is foreseen by measuring the ep inclusive cross section at different incident proton beam energies.

A measurement has been presented of the proton structure function $F_2(x,Q^2)$ in deep inelastic electron-proton scattering at low Q^2 based on data taken in 1995 with the upgraded backward calorimeter and drift chamber. The data cover the region of Q^2 between 0.35 GeV^2 and 3.5 GeV^2 and Bjorken x down to $6\cdot10^{-6}$. The data show a smooth transition from the fixed target high x data to the HERA low x data, and are in accord with the preliminary ZEUS data at very low Q^2 values. The distinct rise of the structure function with decreasing x in the low x region, very prominent for $Q^2 > 2$ GeV^2, diminishes strongly with decreasing Q^2. The rise observed at the smallest values of Q^2 is close to the that expected from Regge parametrizations. A smooth transition from DIS to photoproduction is observed.

References

1. H1 Collab., S. Aid *et al.*, *Nucl. Phys.* B **470**, 3 (1996).
2. ZEUS Collab., M. Derrick *et al.*, DESY preprint 96-76
3. H1 Collab., I. Abt *et al.*, DESY H1-96-01, accepted by Nucl. Instr. and Meth..
4. EMC Collab., J.J. Aubert *et al., Nucl. Phys.* B **231**, 31 (1983).
5. S. Riemersma *et al.*, *Phys. Lett.* B **347**, 143 (1995).
6. M. Glück, E. Reya and A. Vogt, *Z. Phys* **C67**, 433 (1995);
   A. Vogt, Proceedings of the Workshop on Deep-Inelastic Scattering and QCD, Paris (1995) 261.
7. G. Altarelli and G. Martinelli, *Phys. Lett.* B **76**, 89 (1978).
8. H1 Collab., Technical Proposal for the Upgrade of the Backward Region of the H1 Detector, DESY internal report PRC-93/02.
9. E665 Collab., M.R. Adams *et al.*, *Phys. Rev.* D **54**, 3006 (1996).
10. NMC Collab., M. Arneodo *et al.*, *Phys. Lett.* B **364**, 107 (1995).
11. W. Zhu, to appear in the proceedings of the Workshop DIS96, Rome, edt. G. D'Agostini (1996).
12. A. Capella *et al.*, *Phys. Lett.* B **337**, 358 (1994).
13. A. Donnachie and P. V. Landshoff, *Z. Phys.* **C61**, 139 (1994).
14. B. Badelek and J. Kwiecinski, *Phys. Lett.* B **295**, 263 (1992).